ADVANCED FUNCTIONAL MATERIALS
www.afm-journal.de

Near-Infrared Light-Encoded Orthogonally Triggered and Logical Intracellular Release Using Gold Nanocage@Smart Polymer Shell

*Peng Shi, Enguo Ju, Jinsong Ren, and Xiaogang Qu**

Gold nanocages (AuNCs) with hollow interiors, porous walls, and tunable localized surface plasmon resonance (LSPR) peaks in the NIR region represent a promising platform for therapeutic applications, and can be used for orthogonally triggered release by choosing the right laser according to the AuNC's LSPR. AuNCs are prepared with different LSPRs and covered with a smart polymer shell. Laser irradiation in resonance with the LSPR can trigger the release of a pre-loaded effector. As a proof of concept, enzyme and substrate (prodrug) are selectively released from two different AuNCs. Enzymatic reactions only occur after successful opening of both types of AuNC capsules. The system acts as an "AND" logic gate. Furthermore, if the AuNC is loaded with isoenzyme or enzyme inhibitor, an "OR" or "INHIBIT" logic gate operation is achieved. To the best of our knowledge, no reports have combined NIR light-encoded orthogonally triggered release with "prodrug" activation processes to realize defined different logic operations for regulating the dosage of active drug in a specific region. The design is simple and spatial/temporal to control, and provides new insights into developing NIR light-encoded, logically controlled, intracellular release systems.

1. Introduction

Controlled carrier systems have attracted much attention in recent years because of their most important application in high-performance delivery of bioactive substances (drugs, nutrients, contrasts for imaging, genes, etc.), which requires precise spatial and temporal delivery of therapeutic agents to the target site.[1] To date, a number of controlled-release systems have been designed by using a variety of stimuli-responsive "gatekeepers", which can be maneuvered by various stimuli such as salt concentration,[2] pH,[3] temperature,[4] enzyme/DNA,[5] reducing biomolecules,[6] light[7] and so on. Despite these burgeoning developments, most of the designed systems could only respond to a single stimulus and realize release under simple conditions. To prepare an intelligent system that can realize precise control at complicated situations still remains a challenge. Research into smarter and more sophisticated nanocarriers continues to be a very active field.[8]

Molecule-based logic systems and their potential applications are receiving increasing attention.[9] These smart devices give intelligent responses to the external stimuli according to Boolean operations,[10] which are analogous to the digital electronic logic gates on silicon chips. Due to the capability of intelligent judgment, the computation systems can perform multiple operations and precisely process multiple signals (inputs) from the complex environment and generate responses (outputs) autonomously.[11] These insights have lent a strong impetus to the development of more sophisticated controlled release nanodevices. A few groups have reported the application of the logic gate concept to engineer a smart release system, in which biochemical computation performed by DNA,[12] enzymes,[13] or complex biochemical environment[14] would determine the switch of the "releasing gate", which mimics the working principle of the "AND/OR" logic. For therapeutic applications, a physical release mechanism that does not rely on the specific chemical properties of the cellular environment would be highly useful and more easily generalizable to various cell types. Light-induced release is particularly attractive because it can enhance our ability to address the complexity of biological systems by generating effectors with remarkable spatial/temporal resolutions.[7] Recently, Angelos et al. reported dual-controlled nanoparticles by using UV-light and pH inputs.[8] Although promising, ultraviolet/visible light as the input may limit its use in vivo owing to the low penetrability and harm to tissue. The use of lower energy light, near-infrared (NIR) light, has several significant advantages for bioapplications, such as little photodamage to living organisms, good biocompatibility, and high penetration depths in tissues.[15] Therefore, it is highly desirable to develop a NIR light-encoded logic-controlled release system that is simple in design, spatial/temporal to control and promising in vivo application. However, to the best of our knowledge, there is no report to use light-encoded logic gate for controlling intracellular release.

P. Shi, E. Ju, Prof. J. Ren, Prof. X. Qu
Laboratory of Chemical Biology
Division of Biological Inorganic Chemistry
State Key Laboratory of Rare Earth Resource Utilization
Changchun Institute of Applied Chemistry
University of Chinese Academy of Sciences
Chinese Academy of Sciences
Changchun, Jilin 130022, China
E-mail: xqu@ciac.ac.cn

DOI: 10.1002/adfm.201302145

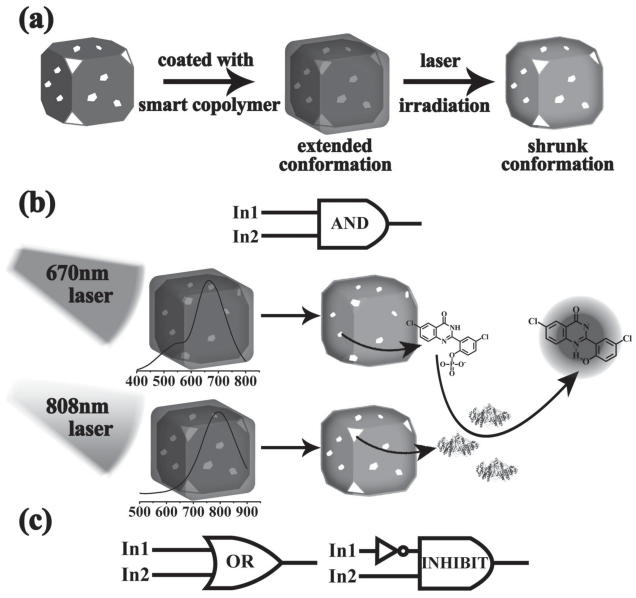

Scheme 1. (a) Illustration of photothermal-sensitive AuNC-copolymer. (b,c) Schematic representation of a NIR light-encoded logic gate for controlled release based on AuNC-copolymer.

Herein, we report a NIR light-encoded orthogonally triggered and logically intracellular release based on gold nanocage@smart polymer shell by combining photothermal-sensitive release and "prodrug" activation process (**Scheme 1**). Gold nanocages (AuNCs) with hollow interiors, porous walls, and tunable localized surface plasmon resonance (LSPR) peaks in the NIR region, represents a new promising platform for therapeutic applications,[16] and can be used for orthogonally triggered release by choosing the right laser. Hollow interiors are suitable for loading not only small molecules but also enzymes.[17] Laser irradiation in resonance with their LSPR can heat AuNCs locally to high temperature through the photothermal effect. Since LSPR is tunable by changing Au/Ag alloy aspect ratio,[18] AuNCs with different LSPR peaks can be excited independently at different wavelengths.[19] If different AuNCs are loaded with different molecules, this strategy can be utilized for orthogonally triggered release of multiple species.[20] However, no reports have combined NIR light-encoded orthogonally triggered release with "prodrug" activation process to realize defined different logic operations for regulating the dosage of "active drug" in a specific region. As shown in Scheme 1, we prepared AuNCs with different LSPR and covered by smart polymer shell. On exposure to a laser beam with a wavelength that matched the absorption peak of the AuNCs, the light would be absorbed and converted into heat. The rise in the local temperature, especially on the surface of AuNCs, would cause the polymer chains to collapse, exposing the pores on the nanocage and thereby releasing the pre-loaded effector. When the laser was turned off, the polymer chains would relax back to the extended conformation and terminate the release. As a proof of concept, we could selectively release enzyme and substrate (prodrug) from two different AuNCs by matching laser excitation wavelength to the AuNC's LSPR. Enzymatic reactions (as observed by onset of fluorescence) only occurred after successful opening of both types of AuNC capsules. The system therefore performed as an "AND" logic gate which generated high output (fluorescent signal) only when both inputs (lasers with different wavelengths) were introduced simultaneously, and no output when either or neither was present. Under "AND" logic operation, the release of "active drug" molecule was controlled by two different NIR lights. Furthermore, it could be used to manually regulate the dosage of active drug in a specific region. The AuNCs were then loaded with isoenzyme or enzyme inhibitor, an "OR" or "INHIBIT" logic gate operation was achieved. Achieving different release windows for each species in a mixture requires engineering intricate architectures. Clearly, such an effective method to externally control release of each species independently and actively could ultimately lead to optimization of therapies for treatment. Our strategy is simple in design, sophisticated to control.

2. Results and Discussion

To realize such a design, AuNC with the LSPR peak at 808 nm covered by poly(*N*-isopropylacrylamide-*co*-acrylamide) (808 nm AuNC–copolymer) was synthesized and well characterized. For pure poly(*N*-isopropylacrylamide), the low critical solution temperature (LCST) was about 32 °C. By incorporating acrylamide into the polymer chain at molar ratio 9:1, we obtained copolymers with LCST at about 39 °C, above the body temperature (37 °C) but below the hyperthermia temperature (42 °C) (**Figure 1**a). After replacing the PVP on nanocage with the smart copolymer, the strong –CO–NH– (1635 cm^{-1}, 1537 cm^{-1}) vibration, which belonged to the copolymer, was observed in the FTIR spectrum (Figure S1a). Below 39 °C, the copolymer is hydrophilic and extended, closing the pores and keeping the loaded species inside the nanocage. When the temperature is raised above the LCST, the copolymer undergoes a phase transition to a shrunk conformation, hydrophobic state, exposing the pores and thereby allowing release (Scheme 1a). As shown in Figure 1b by transmission electron microscope (TEM) imaging, we used 808 nm AuNC of 50 nm in edge length together with a pore size of 5–10 nm, large enough for loading enzyme. The copolymer coating had a relatively uniform thickness of ~4 nm in the dry state. Thermogravimetric analysis (TGA) of AuNC-copolymer showed that there was 14% weight loss up till 450 °C corresponded to the desorption and decomposition of the copolymer (Figure S1c). By dynamic light scattering (Figure 1c), the mean hydrodynamic diameter of the copolymer-covered nanocage was observed to oscillate in response to temperature variation: the diameter decreased on heating to 42 °C and extended to its original value on cooling to 37 °C. These changes with temperature were reversible. We obtained 670 nm AuNC–copolymer using the same methods (Figure S2). UV–vis spectrum validated LSPR peaks were well distributed (Figure 1d).

We first demonstrated selective release dye and enzyme from two different AuNCs to validate feasibility of our design. The 670 nm AuNC–copolymer were added to an aqueous solution of fluorescein and shaken at 42 °C to load the dye. After 12 h, the suspension was quickly cooled to trigger conformational change

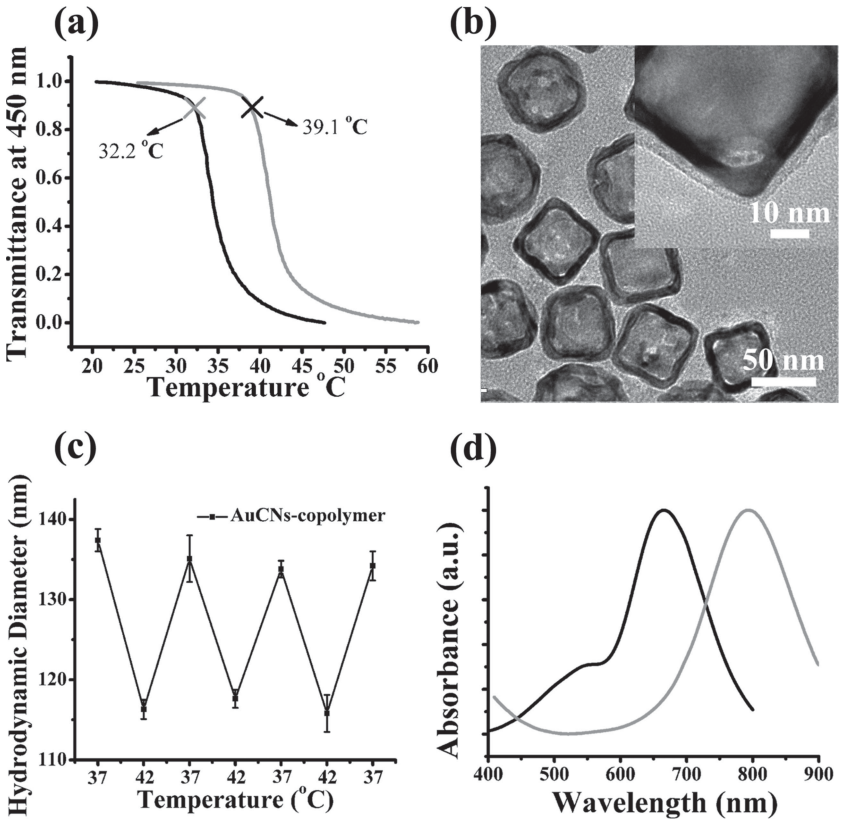

Figure 1. (a) The LCST measured spectrosphotometrically with the solution being heated at a rate of 1 °C/min. The temperature at 90% light transmittance (at 450 nm) of the original polymer solution was defined as the LCST. (b) TEM image of 808 nm AuNC–copolymer. (c) Plots of dynamic light scattering data showing the mean hydrodynamic diameters of 808 nm AuNC–copolymer as a funciton of solution temperature. AuNC–copolymer showed reversible size changes in response to temperature variations. (d) UV–vis spectrum of 670 nm AuNC–copolymer and 808 nm AuNC-copolymer. LSPR peaks were well distributed.

for the copolymer, closing the pores and keeping the loaded dye inside the nanocage. We tested the controlled release with a 670 nm laser by means of the photothermal effect. As shown in **Figure 2**a and b, if the loaded sample was kept under ambient laboratory conditions, the dye remained in the nanocage with negligible release. After the sample exposed to 670 nm laser at 0.4 W/cm^2 for 5 min, the releasing was monitored either by fluorescence or absorbance measurements. Fluorescence at 512 nm increased rapidly illustrating dye release. After that, the fluorescence intensity of the solution remained constant until the sample was again irradiated. More importantly, when the sample was exposed to 808 nm laser, no controlled pulsatile release was observed, which indicated that matching laser excitation wavelength to the LSPR of AuNC was necessary in the open–close protocol. We also obtained the same results (Figure 2c,d) when monitored release process of alkaline phosphatase from 808 nm AuNC–copolymer using UV–vis spectral measurements. Finally, the mixture of 670 nm AuNC–fluorescein–copolymer and 808 nm AuNC–alkaline phosphatase–copolymer was laser irradiated for selective release. After 670 nm irradiation, the supernatant fluorescence at 512 nm increased, illustrating fluorescein release. However, no significant change of absorbance at 280 nm was observed, indicating negligible enzyme release (Figure 2e,f). Therefore, under our experimental conditions, when the sample was exposed to 670 nm laser at 0.4 W/cm^2 for 5 min, 670 nm irradiation could selectively release fluorescein from 670 nm AuNC–copolymer, while leaving 808 nm AuNC–copolymer undisturbed. The low laser power just excited 670 nm AuNC locally and allowed selective release, and therefore had no effect on 808 nm AuNC–copolymer. Negligible temperature increase of the bulk solution, within 2 °C change, was observed after the sample was irradiated by 670 or 808 nm laser at 0.4 W/cm^2 for 5 min (Figure S3a).

Alkaline phosphatase (enzyme 1) converts ELF97 phosphate (substrate) into green fluorescent ELF97 alcohol. Therefore, this enzyme catalytic reaction can be followed by fluorescence change at 517 nm (F517).[21] The highly fluorescent ELF97 alcohol (high F517 value) and non-fluorescent ELF97 phosphate (very low F517 value) could be defined as the reaction ON and OFF states, respectively (**Scheme 2**a). To perform a light-encoded logic gate based on AuNC, we loaded 670 nm AuNC–copolymer with ELF97 phosphate (670 nm AuNC–substrate–copolymer), 808 nm AuNC–copolymer with alkaline phosphatase (808 nm AuNC–enzyme 1–copolymer) and designed an AND logic gate that employs 670 nm laser and 808 nm laser as inputs, fluorescence change as the output. The initial reaction system included 670 nm AuNC–substrate–copolymer and 808 nm AuNC–enzyme 1–copolymer dissolved in Tris-HCl buffer (10 mM, pH 7.0). Scheme 2b and **Figure 3**a showed the signal response after application of different combinations of the laser inputs. In the presence of both inputs (1/1), substrate and enzyme were released and the enzymatic reactions proceeded efficiently, resulting in the formation of ELF97 alcohol. As a result, higher F517 value was obtained (ON state), which was considered as output 1. However, in the absence of either or both of the inputs (0/0, 0/1, 1/0), the enzymatic reactions did not ensue and ELF97 alcohol was not produced. Thus, lower F517 value was detected, that is, logic gate remained in an OFF state (output 0). This system performed AND logic operation corresponding to the Boolean logic multiplication (A•B). Similarly, an OR logic gate could be constructed when introducing acid phosphatase (enzyme 2). Firstly, we should choose an optimum pH which was suitable for both the two isoenzymes. As shown in Figure S4, the logic operations were performed in pH 7.0 Tris-HCl buffer (10 mM) at which alkaline phosphatase was able to maintain ~78% of the bioactivity while acid phosphatase was able to maintain ~57% of the bioactivity. The initial reaction system included substrate, 670 nm AuNC–enzyme 2–copolymer and 808 nm AuNC–enzyme 1–copolymer dissolved in Tris-HCl buffer (10 mM, pH 7.0) (Scheme 2c). ELF97 alcohol could be produced in two parallel biochemical reactions, thus realizing

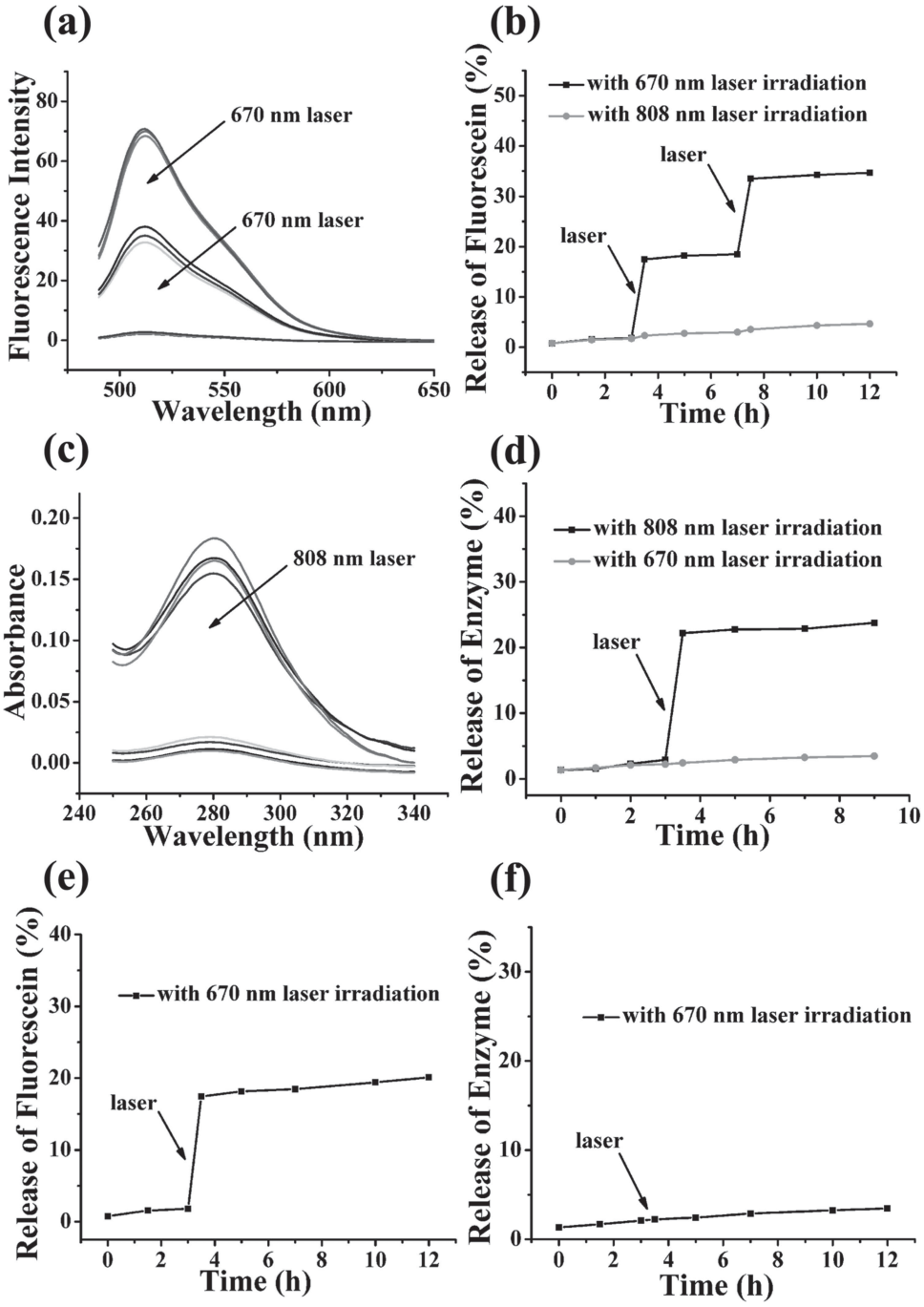

Figure 2. (a,b) Controlled pulsatile release of fluorescein from 670 nm AuNC–copolymer with 670 nm laser (at a power density of 0.4 W/cm^2 for 5 min). In contrast, 808 nm laser did not trigger the release. (a) After 670 nm laser irradiation, fluorescence at 512 nm increased rapidly illustrating fluorescein release. (b) Quantified release efficiency of fluorescein. (c,d) Controlled pulsatile release of alkaline phosphatase from 808 nm AuNC–copolymer with 808 nm laser (at a power density of 0.4 W/cm^2 for 5 min). In contrast, 670 nm laser did not trigger the release. (c) After 808 nm laser irradiation, absorbance at 280 nm increased rapidly illustrating enzyme release. (d) Quantified release efficiency of enzyme. (e,f) Selective release of fluorescein from the mixture of 670 nm AuNC–fluorescein–copolymer and 808 nm AuNC–alkaline phosphatase–copolymer with 670 nm laser. After 670 nm irradiation, (e) release of fluorescein was observed; (f) negligible absorbance change of the enzyme at 280 nm was observed.

the OR logic gate. With no input, none of the biocatalyzed reactions occurred, no fluorescence change was observed, and thus the output of system was "0". In the presence of either or both inputs (1/0, 0/1, 1/1), ELF97 alcohol was produced by either or both enzymatic pathways. As a result, the solution exhibited fluorescence change, which was considered as output 1 (Figure 3b). Therefore, the system could perform OR logic operation, corresponding to the Boolean logic addition: A+B.

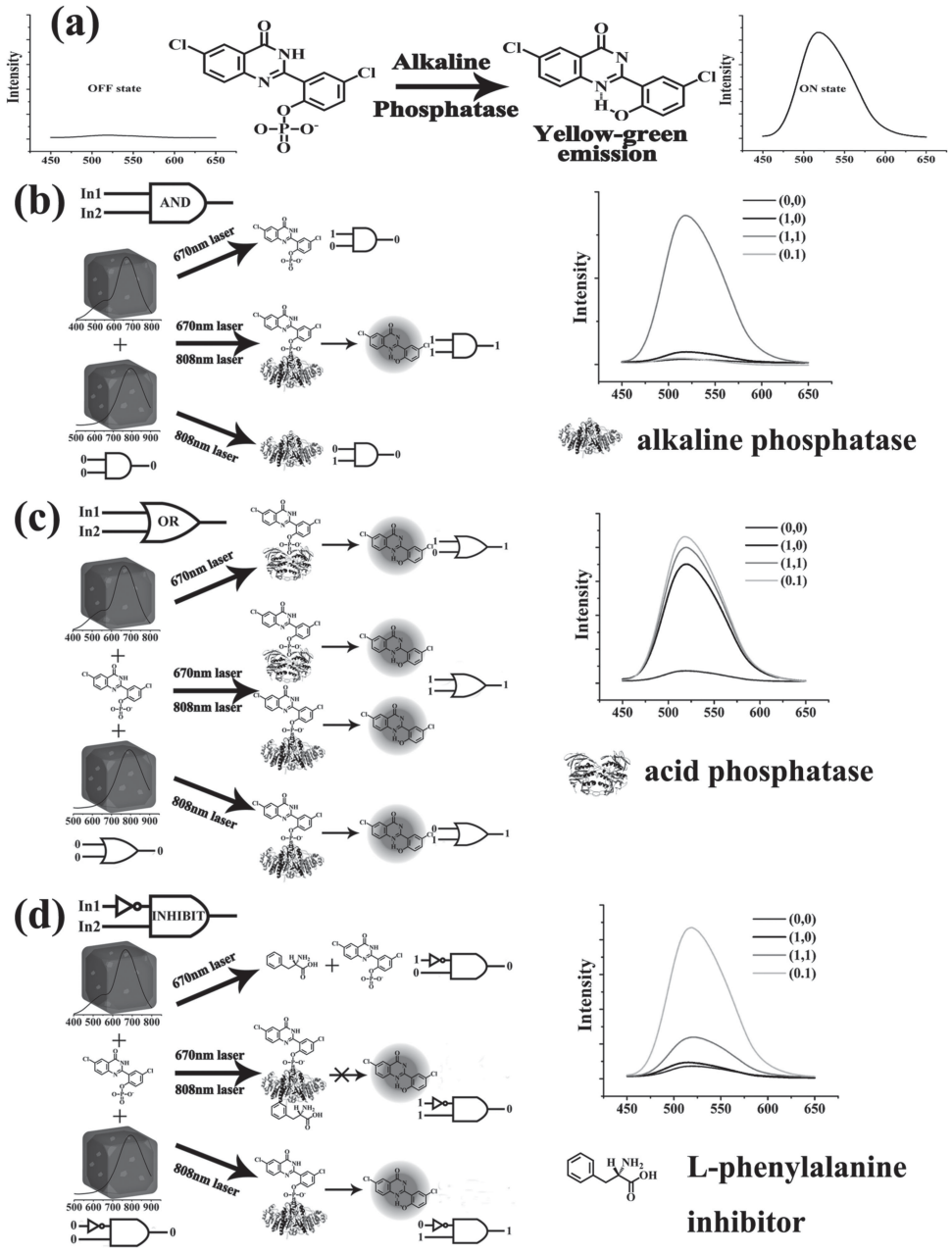

Scheme 2. (a) Schematic representation of the enzymatic reaction. Alkaline phosphatase converts ELF97 phosphate into green fluorescent ELF97 alcohol. Strong fluorescence at 517 nm (F517) was observed. (b–d) Schematic diagrams of our design and operating principle of the "AND", "OR", "INHIBIT" logic gate controlled release systems (b, c, d, respectively).

It could be used to manually regulate the dosage of drug in a specific region. An INHIBIT gate using L-phenylalanine (inhibitor of alkaline phosphatase) was also designed.[22] The initial reaction system included substrate, 670 nm AuNC–inhibitor–copolymer and 808 nm AuNC–enzyme 1–copolymer dissolved in Tris-HCl buffer (10 mM, pH 7.0) (Scheme 2d). 670 nm laser could trigger the release of L-phenylalanine to inhibit enzyme activity and suppress production of fluorescent ELF97 alcohol. When only 808 nm laser was used, the output was 1, otherwise it was 0 (Figure 3c). Taken together, these results demonstrated that our designed system was capable of multiplex logic operations. It is possible to control the release of "active drug" molecule by two different NIR lights and manually regulate the dosage in a specific region.

Most recently, Parak and co-workers designed a light-controlled system to release different molecules. Such a light-mediated release of encapsulated cargo could be used to directly record kinetics of reactions that were triggered by the cargo in the cytosol.[21a] Herein, the success in selective release and light-encoded logic gate prompted us to examine whether our system could work in living cells.[23] To realize NIR light-triggered enzymatic reactions in cells, the feasibility to simultaneously

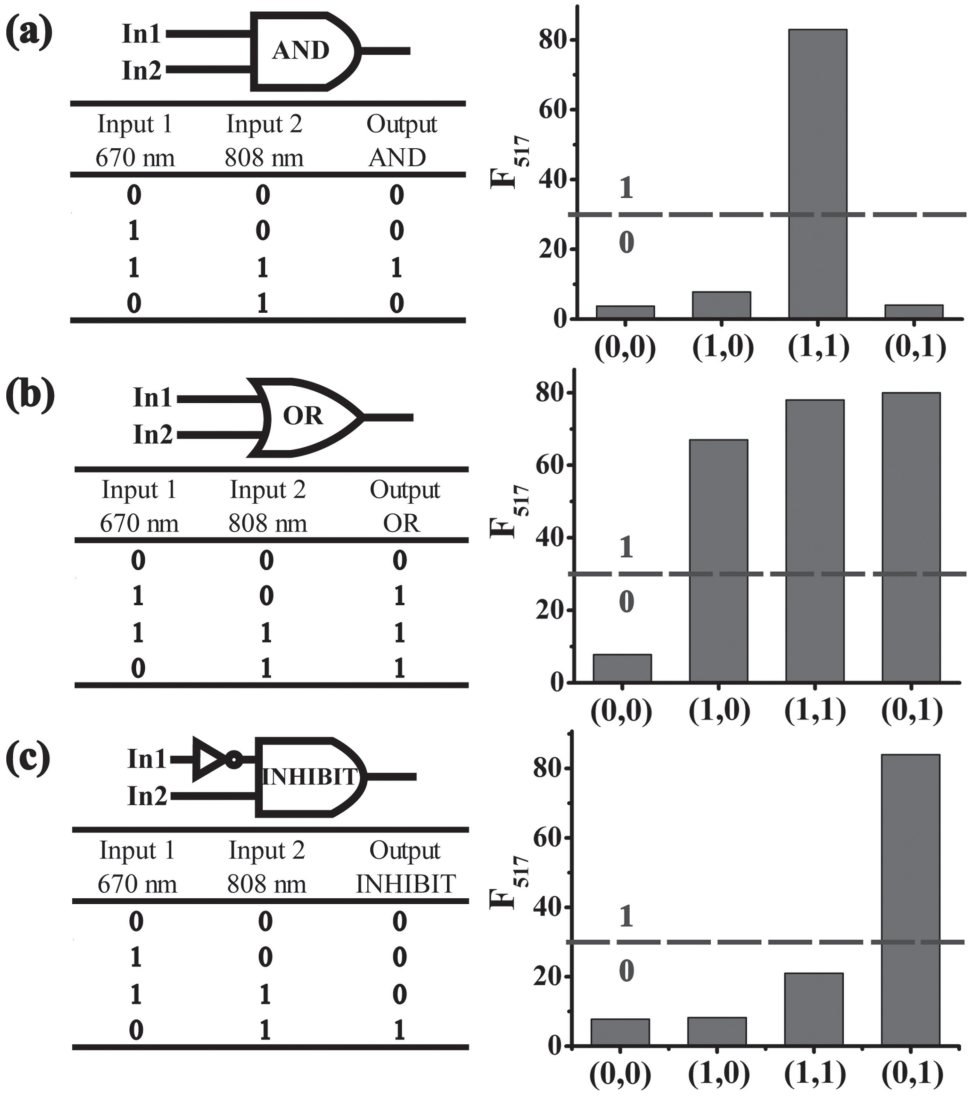

Figure 3. Truth table for (a) AND gate, (b) OR gate and (c) INHIBIT gate. Input 1 is 670 nm laser. Input 2 is 808 nm laser. The output is fluorescence signal at 517 nm. (0,0) (1,0) (1,1) (0,1) are defined as different combinations of the laser inputs.

load cells with a variety of encapsulated cargos is a prerequisite. It is conceivable that if cells are exposed simultaneously to different types of nanodevices with similar layer composition, they will internalize them with a statistical distribution.[21a] To demonstrate this, we exposed A549 cells to a mixture of 670 nm AuNC–copolymer and 808 nm AuNC–copolymer, which were equivalent in amounts, loaded with fluorescein and Rhodamine B, respectively. After incubation for 5 h, the culture media was replaced by fresh media and the cells were subjected to different laser irradiations. The cells were further incubated for 1 h and then imaged using confocal laser scanning microscope. As shown in **Figure 4**, the green fluorescence from fluorescein and red fluorescence from Rhodamine B could be clearly observed in the cytoplasmic region in one cell, demonstrating that 670 nm AuNC–copolymer and 808 nm AuNC-copolymer had been taken up by A549 cells. In contrast, just green or red signal could be seen if A549 cells were exposed to 670 nm AuNC–fluorescein–copolymer or 808 nm AuNC–Rhodamine B–copolymer, respectively (**Figure 5**). We should note that low laser intensity as we used had no effect on cell viability (Figure S5).

Base on the above results, we next performed a light-encoded "AND" logic gate for triggering of an enzymatic reaction in living cells. 670 nm AuNC–substrate–copolymer and 808 nm AuNC–enzyme 1–copolymer were delivered into the same cell and independently opened with different laser. As a result, the contents of the AuNC capsules (the enzyme or the substrate) were released into the cytosol. When just the substrate or the enzyme was released by light-controlled opening of one of the AuNC–copolymer, no fluorescence change was observed (**Figure 6**). However, after opening of both types of AuNC–copolymer, substrate and enzyme were released and the enzymatic reactions proceeded efficiently, resulting in the formation of ELF97 alcohol, as observed by the green fluorescence in the cytosol. With different combinations of the laser inputs, we got different signal responses in the cells, indicating the system has performed "AND" logic operation.

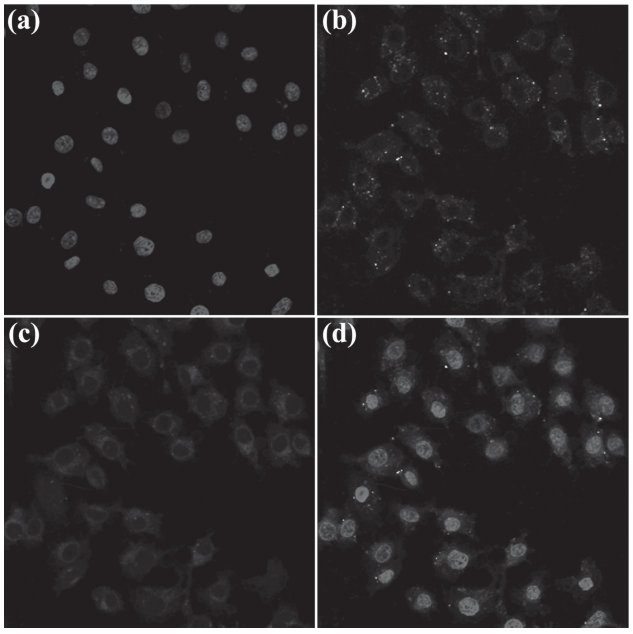

Figure 4. Confocal laser scanning microscopy (CLSM) images of A549 cells incubated with 670 nm AuNC–fluorescein–copolymer and 808 nm AuNC–Rhodamine B–copolymer for 5 h and then irradiated by lasers. The images can be classified to (a) the nuclei of cells (being dyed in blue by Hoechst 33324), (b) green fluorescence from fluorescein, (c) red fluorescence from Rhodamine B, and (d) the merged images of all above, respectively.

3. Conclusion

Combining NIR light-encoded orthogonally triggered release with "prodrug" activation process, we report the first example of NIR light-encoded orthogonally triggered and logically intracellular release based on gold nanocage@smart polymer shell. By using defined logic operation, and tunable LSPR property of AuNC, a sophisticated release system can be realized. Under "AND" logic operation, the release of active drug molecule is controlled by two different NIR lights. Under "OR" "INHIBIT" logic operation, it is possible to manually regulate the dosage in a specific region. Our design is simple and spatial/temporal to control, and would provide new insights into developing NIR light-encoded, logically controlled intracellular release system.

4. Experimental Section

Materials and Instrumentation: The monomer, *N*-isopropylacrylamide (NIPAAm, 99%) was obtained from Sigma-Aldrich and recrystallized in hexane prior to use. Acrylamide (AAm, 99%) was purchased from Sigma-Aldrich and recrystallized in methanol before use. $AgNO_3$ (more than 99%), PVP (powder, average Mr 29 000 or 55 000), $HAuCl_4$–$3H_2O$ (99.9+%), 4-(dimethylamino)pyridine (DMAP), Copper(I) bromide (CuBr), *N,N,N′,N′,N′*-pentamethyldiethylenetriamine (PMDETA), *N,N′*-dicyclohexylcarbodiimide (DCC) and 2-bromoisobutyric acid were all obtained from Sigma-Aldrich and used as received. (Bis(2-hydroxyethyl) disulfide (BHEDS; 90%) was purchased from Alfa Aesar. Tetrahydrofuran (THF), dimethyl sulfoxide (DMSO), ethylene glycol, and ethanol were all purchased from Beijing Chemicals (Beijing, China). ELF97 phosphatase substrate was obtained from Invitrogen. Alkaline phosphatase from bovine intestinal mucosa was purchased from New England Biolabs. Acid phosphatase from potato was purchased from Sigma-Aldrich. Nanopure water (18.2 MΩ/cm, Millpore Co., USA) was used in all experiments and to prepare all buffers.

Fourier-transform infrared spectrophotometer (FTIR) analyses were carried out on a Bruker Vertex 70 FT-IR Spectrometer. Transmission electron microscopy (TEM) images were recorded using a FEI TECNAI G2 20 high-resolution transmission electron microscope operating at 100 kV. UV–vis spectroscopy was carried out with a JASCO V-550 UV/vis spectrometer. Fluorescence measurements were carried out on a JASCO FP-6500 spectrofluorometer. Dynamic light scattering (DLS) measurements were performed on a Malvern Zetasizer NanoS apparatus equipped with a 4.0 mW laser operating at $\lambda = 633$ nm. All samples were measured at a scattering angle of 90° with particle concentration of about 0.2 mg/mL at 25 °C. A CWdiode laser with wavelength of 808 nm and 670 nm were used for the laser irradiation experiment.

Synthesis of Poly(N-isopropylacrylamide-co-acrylamide): The disulfide-containing initiator, bis(2-hydroxyethyl)disulfide bis(2-bromo propionate) ($BHEDS(BP)_2$) was firstly synthesized according to the literature.[24] 10.05 g (0.065 mol) of BHEDS was dissolved in 175 mL of THF. A solution of 21.7 g (0.13 mol) of 2-bromoisobutyric acid in 25 mL of THF was added, and the solution was cooled in an ice-water bath. A solution of 26.83 g (0.13 mol) of DCC in 25 mL of THF was added upon stirring followed by a solution of 1.6 g of 4-DMAP in 25 mL of THF. The reaction mixture was kept in the ice-water bath for 5 min and then for 18 h at room temperature. The precipitated dicyclohexylcarbamide was filtered off and washed with 25 mL of THF on the filter. The solvent was evaporated, and the formed suspension was kept in refrigerator for several hours and then at room temperature for 3 days. The impurities crystallized and were removed by filtration. ^{1}H NMR (methanol-d_4): 4.57–4.38 ppm (slightly overlapping q, 1H, CHBr, and t, 2H, CH_2O), 3.02 ppm (t, 2H, CH_2S), and 1.80 ppm (d, 3H, CH_3). Based on analysis of the spectrum, approximately 2% of unreacted diol remained after the esterification reaction. (The signals of the diol dissolved in methanol-d_4

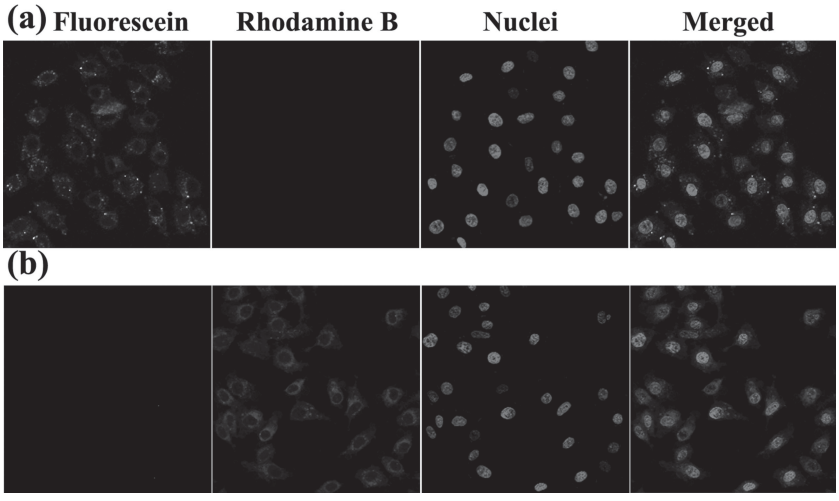

Figure 5. Confocal laser scanning microscopy (CLSM) images of A549 cells incubated with (a) 670 nm AuNC–fluorescein–copolymer or (b) 808 nm AuNC–Rhodamine B–copolymer for 5 h, and irradiated by lasers.

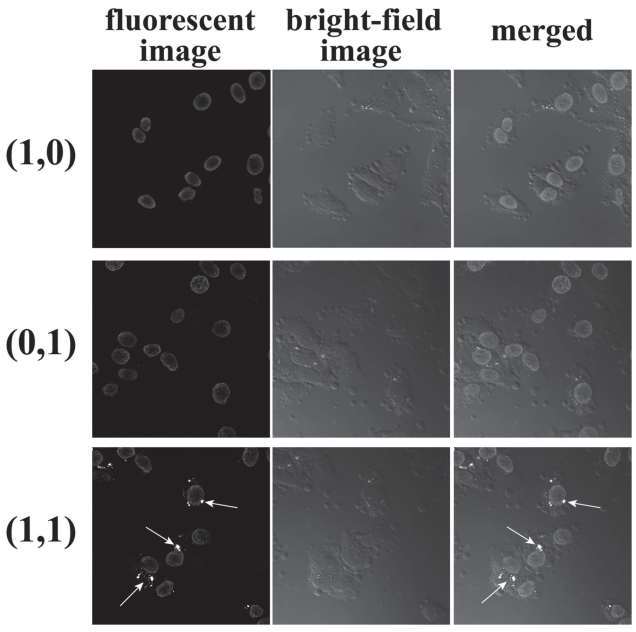

Figure 6. A NIR light-encoded "AND" logic gate for triggering of an enzymatic reaction in living cells. A549 cells were incubated with 670 nm AuNC-substrate-copolymer+808 nm AuNC-enzyme 1-copolymer for 5 h and irradiated by different combinations of the laser inputs. (1,0) Only 670 nm laser is present triggering the release of substrate. (0,1) Only 808 nm laser is present triggering the release of enzyme 1, (1,1) Both 670 nm laser and 808 nm laser are present triggering the release of substrate and enzyme 1, resulting in enzymatic reaction.

are situated at 4.73 ppm (broad m, 1H, OH), 3.80 ppm (t, 2H, CH_2O), and 2.84 ppm (t, 2H,CH_2S).)

NIPAAm (2.0 g), PMDETA (35 µl), $BHEDS(BP)_2$ (0.015 g), deionized water (18 mL) and methanol (12 mL) were mixed in a Schlenk flask and degassed by freeze-pump-thaw cycles. While the mixture was frozen, CuBr (0.010 g) was added. The flask was then filled with argon and the mixture was left to melt at room temperature. The reaction solution was magnetically stirred overnight at room temperature. After evaporation of the solvent, the crude product was dissolved in water and purified by dialysis to yield pNIPAAm (NIPAAm (90%, 1.83 g) and AAm (10%, 0.13 g) for an LCST at 39 °C).

Synthesis of Gold Nanocage (AuNC): AuNC were synthesized by means of the galvanic replacement reaction between Ag nanocubes and $HAuCl_4$ according to a previously reported method.[18] Briefly, 500 µL of the Ag nanocubes (3 nM) was added to 5 mL of deionized water containing poly (vinyl pyrrolidone) (PVP, 1 mg/mL) hosted in a 50 mL flask under magnetic stirring and then heated to boil for 10 min. In the meantime, an aqueous solution of $HAuCl_4$ (0.5 mM) was prepared. The $HAuCl_4$ was added to the flask at a rate of 45 mL/h until the solution had a desired optical extinction peak as confirmed by UV spectroscopy. The solution was refluxed for another 30 min until the color of the reaction was stable. Once cooled to room temperature, the sample was centrifuged and washed with saturated NaCl solution to remove AgCl and with water several times to remove PVP and NaCl.

Exchange of PVP with Copolymer: The as-synthesized PVP-covered Au nanocage were dispersed in 2 mL of deionized water and added to a 20 mL aqueous solution of copolymer (0.20 g). The mixture was shaken at 800 rpm for three days. The solution was then centrifuged at 12 000 rpm and the supernatant was discarded. The polymer-covered Au nanocage was washed three more times with 2 mL (each time) of deionized water.

Loading the Nanocage with Fluorescein, Rhodamine B, ELF97 Phosphate, L-Phenylalanine, Alkaline Phosphatase or Acid Phosphatase: The AuNC-copolymer was added to an aqueous solution containing fluorescein (0.2 mM), Rhodamine B (0.2 mM), ELF97 phosphate (0.5 mM, 5%DMSO), L-phenylalanine (0.2 mM), alkaline phosphatase (5.0 units/mL) or acid phosphatase (3.0 units/mL) respectively. The obtained mixture was shaken overnight at 1000 rpm at 42 °C. The mixture was then cooled with an ice bath for 0.5 h, and centrifuged at 12 000 rpm for 15 min. Finally, the supernatant was decanted and the loaded samples were washed three times with deionized water. All the washing solutions were collected, and the loading of ELF97 phosphate (alkaline phosphatase) was calculated from the difference in the concentration of the initial and left ELF97 phosphate (alkaline phosphatase). The loading capability is 28.5 µg ELF97 phosphate/mg AuNC and 53 µg alkaline phosphatase /mg AuNC.

Selective Releasing Dye or Enzyme from Gold Nanocage by Laser: Taking the dye release as an example (the release experiments were performed in room temperature), AuNC-fluorescein-copolymer was dispersed in PBS (10 mM, pH 7.4). The sample was then exposed to 670 nm laser at 0.4 W/cm^2 for 5 min. After exposure, aliquots were taken from the suspension the solution and were centrifuged at 12,000 rpm for 15 min, and the supernatant was collected for fluorescence spectral measurement. The delivery of dye from the pore to the buffer solution was monitored via the fluorescence at 512. 808 nm AuNC-enzyme-copolymer was exposed to 808 nm laser at 0.4 W/cm^2 for 5 min. The delivery of enzyme from the pore to the buffer solution was monitored via the absorbance band at 280 nm.

AuNC-Copolymer Based Logic Operations in Solution: Taking the AND gate as an example, the initial reaction system included 670 nm AuNC-substrate-copolymer and 808 nm AuNC-enzyme 1-copolymer dissolved in Tris-HCl buffer (10 mM, pH 7.0). After exposure to different combinations of the laser inputs (0/0, 0/1, 1/0, 1/1), the solution was centrifuged at 12 000 rpm for 15 min. The supernatant was cultured at 37 °C for 30 min and then measured with fluorescence spectral (the excitation wavelength was 350 nm). For each gate, the amounts of 670 nm AuNC–substrate–copolymer and 808 nm AuNC–enzyme 1–copolymer were first roughly estimated and then optimized in order to get a significant difference of F517 between the states "0" and "1". For the OR gate, the initial system included substrate (0.1 µmol/mL), 670 nm AuNC–enzyme 2–copolymer and 808 nm AuNC–enzyme 1–copolymer dissolved in Tris-HCl buffer (10 mM, pH 7.0). For the INHIBIT gate, the initial reaction system included substrate (0.1 µmol/mL), 670 nm AuNC–inhibitor–copolymer and 808 nm AuNC–enzyme 1–copolymer dissolved in Tris-HCl buffer (10 mM, pH 7.0).

Cell Culture: Human lung adenocarcinoma A549 cells were cultured in 25 cm^2 flasks in Dulbecco's Modified Eagle's Medium DMEM (Gibco) containing 10% (v/v) fetal bovine serum (Gibco) at 37 °C in an atmosphere of 5% (v/v) CO_2 in air. The media were changed every three days, and the cells were passaged by trypsinization before confluence.

Inductively Coupled Plasma Mass Spectrometry (ICP-MS) Measurement: To quantitatively measure the AuNC–copolymer uptake by A549 cells, ICP-MS measurement was carried out. A549 cells were cultured at a density of 3.0×10^6 cells per flask for 24 h. The media was then removed and replaced with 4 mL of fresh media containing 1 mg AuNC–copolymer. The flasks were incubated for 5 h and then washed with PBS 5 times. Finally, the cells were lysed by cell lysis buffer. Au contents in the cell lysis solution were determined by ICP-MS. The obtained result suggested that the efficiency of AuNC-copolymer internalization by A549 cells was about 63%.

Fluorescence Imaging: A549 cells were seeded in a 24-well plate and cultured for 24 h. The cell medium was removed, and then cells were incubated with 0.5 mL of fresh cell medium containing 30 µg 670 nm AuNC-fluorescein-copolymer or 30 µg 808 nm AuNC-Rhodamine B-copolymer or 20 µg 670 nm AuNC–fluorescein–copolymer+20 µg 808 nm AuNC–Rhodamine B–copolymer for 5 h. For intracellular enzymatic reaction, the cells were incubated with 0.5 mL of fresh cell medium containing 30 µg 670 nm AuNC–substrate–copolymer+30 µg 808 nm AuNC–enzyme 1–copolymer for 5 h. After that, the culture media was

replaced by fresh media and the cells were subjected to different laser irradiation. The cells were further incubated for 1 h and then imaged using confocal laser scanning microscope.

In Vitro Cytotoxicity Assay: For studying the cytotoxicity, A549 cells were seeded in a 96-well plate at a density 10^4 cells/well for 24 h at 37 °C in 5% CO_2. Then, the cells were treated with AuNC–copolymer at desired concentration. After maintained for 6 h, the plates were photo-irradiated by a laser lamp (λ = 670 nm, 0.4 W/cm^2 or 808 nm, 0.4 W/cm^2) for 5 min. After further incubation for 24 h, cell viabilities were tested by standard MTT (3-(4, 5)-dimethylthiahiazo-2-yl)-2, 5-diphenyltetrazolium bromide) assay.

Supporting Information

Supporting Information is available from the Wiley Online Library or from the author.

Acknowledgements

Financial support was provided by 973 Project (2011CB936004, 2012CB720602), and NSFC (221210002, 91213302).

Received: June 24, 2013
Revised: July 19, 2013
Published online: September 3, 2013

[1] a) E. Aznar, R. Martínez-Máñez, F. Sancenón, *Expert. Opin. Drug Deliv.* **2009**, *6*, 643; b) O. C. Farokhzad, R. Langer, *ACS Nano* **2009**, *3*, 16; c) M. Vallet-Regí, F. Balas, D. Arcos, *Angew. Chem. Int. Ed.* **2007**, *46*, 7548; d) C.-Y. Lai, B. G. Trewyn, D. M. Jeftinija, K. Jeftinija, S. Xu, S. Jeftinija, V. S. Y. Lin, *J. Am. Chem. Soc.* **2003**, *125*, 4451; e) M. V. Risbud, A. A. Hardikar, S. V. Bhat, R. R. Bhonde, *J. Control. Release* **2000**, *68*, 23; f) L. Yu, J. Ding, *Chem. Soc. Rev.* **2008**, *37*, 1473.

[2] K. C. F. Leung, T. D. Nguyen, J. F. Stoddart, J. I. Zink, *Chem. Mater.* **2006**, *18*, 5919.

[3] a) R. Liu, Y. Zhang, X. Zhao, A. Agarwal, L. J. Mueller, P. Feng, *J. Am. Chem. Soc.* **2010**, *132*, 1500; b) W. Wang, D. Cheng, F. Gong, X. Miao, X. Shuai, *Adv. Mater.* **2012**, *24*, 115.

[4] Y.-Z. You, K. K. Kalebaila, S. L. Brock, D. Oupický, *Chem. Mater.* **2008**, *20*, 3354.

[5] a) C. Chen, J. Geng, F. Pu, X. Yang, J. Ren, X. Qu, *Angew. Chem. Int. Ed.* **2011**, *50*, 882; b) N. Singh, A. Karambelkar, L. Gu, K. Lin, J. S. Miller, C. S. Chen, M. J. Sailor, S. N. Bhatia, *J. Am. Chem. Soc.* **2011**, *133*, 19582.

[6] T. D. Nguyen, Y. Liu, S. Saha, K. C. F. Leung, J. F. Stoddart, J. I. Zink, *J. Am. Chem. Soc.* **2007**, *129*, 626.

[7] a) B. Yan, J.-C. Boyer, N. R. Branda, Y. Zhao, *J. Am. Chem. Soc.* **2011**, *133*, 19714; b) N. K. Mal, M. Fujiwara, Y. Tanaka, *Nature* **2003**, *421*, 350; c) B. P. Timko, T. Dvir, D. S. Kohane, *Adv. Mater.* **2010**, *22*, 4925.

[8] S. Angelos, Y.-W. Yang, N. M. Khashab, J. F. Stoddart, J. I. Zink, *J. Am. Chem. Soc.* **2009**, *131*, 11344.

[9] a) P. A. de Silva, N. H. Q. Gunaratne, C. P. McCoy, *Nature* **1993**, *364*, 42; b) L. Adleman, *Science* **1994**, *266*, 1021.

[10] a) Y. Benenson, B. Gil, U. Ben-Dor, R. Adar, E. Shapiro, *Nature* **2004**, *429*, 423; b) A. P. De Silva, *Nat. Mater.* **2005**, *4*, 15.

[11] a) S. Bi, Y. Yan, S. Hao, S. Zhang, *Angew. Chem. Int. Ed.* **2010**, *49*, 4438; b) Y. Lin, C. Xu, J. Ren, X. Qu, *Angew. Chem. Int. Ed.* **2012**, *51*, 12579.

[12] a) S. M. Douglas, I. Bachelet, G. M. Church, *Science* **2012**, *335*, 831; b) Y. Wen, L. Xu, C. Li, H. Du, L. Chen, B. Su, Z. Zhang, X. Zhang, Y. Song, *Chem. Commun.* **2012**, *48*, 8410.

[13] a) R. J. Amir, M. Popkov, R. A. Lerner, C. F. Barbas, D. Shabat, *Angew. Chem. Int. Ed.* **2005**, *44*, 4378; b) V. Bocharova, O. Zavalov, K. MacVittie, M. A. Arugula, N. V. Guz, M. E. Dokukin, J. Halamek, I. Sokolov, V. Privman, E. Katz, *J. Mater. Chem.* **2012**, *22*, 19709.

[14] a) M. Zhou, N. Zhou, F. Kuralay, J. R. Windmiller, S. Parkhomovsky, G. Valdés-Ramírez, E. Katz, J. Wang, *Angew. Chem. Int. Ed.* **2012**, *51*, 2686; b) H. Komatsu, S. Matsumoto, S.-i. Tamaru, K. Kaneko, M. Ikeda, I. Hamachi, *J. Am. Chem. Soc.* **2009**, *131*, 5580; c) C. Wei, J. Guo, C. Wang, *Macromol. Rapid Commun.* **2011**, *32*, 451; d) E. A. Mahmoud, J. Sankaranarayanan, J. M. Morachis, G. Kim, A. Almutairi, *Bioconjug. Chem.* **2011**, *22*, 1416.

[15] a) G. Wu, A. Mikhailovsky, H. A. Khant, C. Fu, W. Chiu, J. A. Zasadzinski, *J. Am. Chem. Soc.* **2008**, *130*, 8175; b) Y.-T. Chang, P.-Y. Liao, H.-S. Sheu, Y.-J. Tseng, F.-Y. Cheng, C.-S. Yeh, *Adv. Mater.* **2012**, *24*, 3309; c) X. Yang, X. Liu, Z. Liu, F. Pu, J. Ren, X. Qu, *Adv. Mater.* **2012**, *24*, 2890; d) C.-C. Chen, Y.-P. Lin, C.-W. Wang, H.-C. Tzeng, C.-H. Wu, Y.-C. Chen, C.-P. Chen, L.-C. Chen, Y.-C. Wu, *J. Am. Chem. Soc.* **2006**, *128*, 3709.

[16] Y. Xia, W. Li, C. M. Cobley, J. Chen, X. Xia, Q. Zhang, M. Yang, E. C. Cho, P. K. Brown, *Acc. Chem. Res.* **2011**, *44*, 914.

[17] a) M. S. Yavuz, Y. Cheng, J. Chen, C. M. Cobley, Q. Zhang, M. Rycenga, J. Xie, C. Kim, K. H. Song, A. G. Schwartz, L. V. Wang, Y. Xia, *Nat. Mater.* **2009**, *8*, 935; b) G. D. Moon, S.-W. Choi, X. Cai, W. Li, E. C. Cho, U. Jeong, L. V. Wang, Y. Xia, *J. Am. Chem. Soc.* **2011**, *133*, 4762; c) P. Shi, K. Qu, M. Li, J. Wang, J. Ren, X. Qu, *Chem. Commun.* **2012**, *48*, 7640; d) P. Shi, M. Li, J. Ren, X. Qu, *Adv. Funct. Mater.* **2012**, DOI: 10.1002/adfm.201301015.

[18] S. E. Skrabalak, L. Au, X. Li, Y. Xia, *Nat. Protoc.* **2007**, *2*, 2182.

[19] a) A. Wijaya, S. B. Schaffer, I. G. Pallares, K. Hamad-Schifferli, *ACS Nano* **2008**, *3*, 80; b) S. R. Sershen, G. A. Mensing, M. Ng, N. J. Halas, D. J. Beebe, J. L. West, *Adv. Mater.* **2005**, *17*, 1366.

[20] a) S. J. Leung, X. M. Kachur, M. C. Bobnick, M. Romanowski, *Adv. Funct. Mater.* **2011**, *21*, 1113; b) S. E. Lee, G. L. Liu, F. Kim, L. P. Lee, *Nano Lett.* **2009**, *9*, 562; c) A. G. Skirtach, P. Karageorgiev, B.G. De Geest, N. Pazos-Perez, D. Braun, G. B. Sukhorukov, *Adv. Mater.* **2008**, *20*, 506.

[21] a) M. Ochs, S. Carregal-Romero, J. Rejman, K. Braeckmans, S. C. De Smedt, W. J. Parak, *Angew. Chem. Int. Ed.* **2013**, *52*, 695; b) J. Nedoma, A. Štrojsová, J. Vrba, J. Komárková, K. Šimek, *Environ. Microbiol.* **2003**, *5*, 462.

[22] K. Watanabe, W. H. Fishman, *J. Histochem. Cytochem.* **1964**, *12*, 252.

[23] A. G. Skirtach, A. Muñoz Javier, O. Kreft, K. Köhler, A. Piera Alberola, H. Möhwald, W. J. Parak, G. B. Sukhorukov, *Angew. Chem. Int. Ed.* **2006**, *45*, 4612.

[24] N. V. Tsarevsky, K. Matyjaszewski, *Macromolecules* **2005**, *38*, 3087.